

Manuscript Number: GEOMOR-1941R1

Title: Assessing debris flows using LIDAR differencing: 18th May 2005 Matata event, New Zealand

Article Type: Research Paper

Keywords: LIDAR differencing, slope failure, debris flow, sediment pathways, Matata, hazard assessment, LIDAR

Corresponding Author: Professor Jonathan Bull,

Corresponding Author's Institution: University of Southampton

First Author: Jonathan Bull

Order of Authors: Jonathan Bull; Helen Miller; Darren M Gravley; Daniel Costello; Daniel C Hikuroa; Justin K Dix

Abstract: The town of Matata in the Eastern Bay of Plenty (New Zealand) experienced an extreme rainfall event on the 18th of May 2005. This event triggered widespread landslips and large debris flows in the Awatarariki and Waitepuru catchments behind Matata. LIDAR (Light Detection and Ranging technology) data sets flown prior to and following this event have been differenced and used in conjunction with a detailed field study to identify the distribution of debris and major sediment pathways which, from the Awatarariki catchment, transported at least $350,000 \pm 50,000$ m³ of debris. Debris flows were initially confined to stream valleys and controlled by the density and hydraulic thrust of the currents, before emerging onto the Awatarariki debris fan where a complex system of unconfined sediment pathways developed. Here, large boulders, clasts, logs and entire homes were deposited as the flows decelerated. Downstream from the debris fan, the pre-existing coastal foredune topography played a significant role in deflecting the more dilute currents that in filled lagoonal swale systems in both directions. The differenced LIDAR data has revealed several sectors characterised by significant variation in clast size, thickness and volume of debris as well as areas where post-debris flow cleanup and grading operations have resulted in man-made levees, sediment dumps, scoured channels and substantial graded areas. The application of differenced LIDAR data to a debris flow event demonstrates the techniques potential as a precise and powerful tool for hazard mapping and assessment.

School of Ocean and Earth Sciences
University of Southampton
National Oceanography Centre Southampton
Southampton SO14 3ZH
U.K.

Email: jmb1@noc.soton.ac.uk

16th August 2010

Takashi OGUCHI
Co-Editor-in-Chief: Geomorphology (Elsevier)

Dear Takashi,

Revised Manuscript for Geomorphology - Ms. Ref. No.: GEOMOR-1941. Title: Assessing debris flows using LIDAR differencing: 18th May 2005 Matata event.

Thank you for your and the two reviewers comments. I have now completed the revisions and uploaded the manuscript

With regard to the figures I have combined Figures 9 and 10 into a new Figure 9. This was to simplify and enable the reader to see the whole area that has been differenced. Figures 3 and 7 are provided as both black/white and colour so that the colour can be used on-line. We now have three colour figures (2, 8 and 9).

I indicate below in detail how we have responded to the detailed comments on the manuscript. Please do not hesitate to contact us if you require more information.

Yours sincerely
Jon

Professor Jonathan Bull

Response to Reviewers' comments:

Responses are indicated in italics.

Reviewer #1:

line 26: add (New Zealand) after Plenty – *Done*.

line 42: The last sentence of the abstract is too general. The impact of the debris flow has been assessed in this paper. – *We have amended the last sentence to make this clear.*

-line 70: I think that a great advantage of the LIDAR is that it gives a synoptic view of large areas. That is not the case of conventional geodetic techniques. – *A useful comment – sentence added at line 80-81*

-line 102 to 114: the parts 2 and 3 could be presented in an other way. I think that you could be more precise on rainfalls, topography and geology in the part 2. For example, you indicate the thickness of the ignimbrite in part 3. You could also precise if historic debris flows have occurred.

We don't agree with these comments. The Regional Geologic Setting section is exactly that, it lays down the regional context and highlights some important detail that is referred to throughout the paper (i.e. the Matahina ignimbrite whose distribution is not only regional in scale but it is an important lithology in the debris flow story).

-fig 3 not necessary, or can be completed by a 3D view of the geology -This figure gives the reader a much better vision of the field area, the scale of the coastal cliffs and a perspective on the source and sink of the debris flows relative to the township of Matata.

-fig 7: there is a problem in the overlap of the aerial images, mainly for the two western bands. This is a very minor point. There is a small issue, hopefully partially resolved by better presentation of new Fig 7.

fig 8: the scale of Height is too small and difficult to read. Scale now bigger

table 2 and discussion: Could you add explicitly the surface covered by the debris flow ? How is estimated the error for the total volume ? from the error bar on the LIDAR data ? We are not keen to add surface area as we do not think it a significant parameter – volume is most important. Errors are discussed in the text.

Reviewer #2:

Lines 115-478: Sources of descriptions are not clear. The title of the section is "Eyewitness, Photo and Field Observation of ...". It is not clear descriptions are based either on Eyewitness, Photo, or Field Observation. It is preferable for the authors to indicate this point in the text.

I have added text to show, specifically, the source of the descriptions.

Line 124: Is the return period 500 years obtained from a calculation by the authors or referred to other data from e.g. an agency of meteorological survey? How long: how many years is the duration of actual rainfall observation data for the calculation of the rainfall return period for this gauging site?

I have sited the reference for the 500 year return period in the text and I have also added a sentence to explain how it was obtained. It is a probability thing as opposed to records of similar intense rainfall events. In other words it is possible that a similar rainfall event could occur in less than 500 years.

Lines 124, 167, and 172: Is it appropriate to use "c." instead of the term "about" in the manuscript of original article? We see no problem with using c. – please advise otherwise.

Line 175: Description "100s of m" is hard to be understood. Now sorted.

Line 210: Is the location of the description "(Fig. 7)" is appropriate in the sentence? Now removed

Line 216: Why you say "are not significant"? I think it preferable to say "are meaningless". Changed.

Line 222: Please supply the exact acquisition dates of LIDAR data and the aerial photography data. It would be necessary that there are no significant changes in the topography of the study terrains between two data sets.

We have included dates for LIDAR, there is some uncertainty about photo dates, but we know they pre-date the debris flow event.

Lines 274-276: The authors indicate "the presence of irregular fingers of higher elevation. Is it capable to differentiate those deposits from "debris lobe" or "debris-flow lobe" which were defined and used by e.g. Hooke (1967), Johnson (1970), Lowe (1976), Pierson (1980) and Suwa and Okuda (1983)?

These fingers may very well be debris lobes but post debris-flow cleanup makes it difficult to ground-truth these features (i.e. measure the dimensions, morphology and grainsize distribution of these features). In addition, where we mention these in this section we are trying to demonstrate observations that can be made from the Lidar differenced data and not interpret the processes responsible for there formation. Later in the Discussion section we do provide some interpretations of the processes based on a comparison of field, photo and Lidar data (i.e. the formation of the broad fan area and the lobate structure at the distal margins as well as the smaller fan structures emanating from the front of the broad fan.

Lines 338-341: Source of the data described should be referred here in the text. *Done.*

Line 396: Why "?" is attached to "Hayden Reed"? Is it appropriate? *Question now removed*

Line 397: What does "HM" mean? *Sorted*

Line 493: Indication of the exact date of the image would be preferable. *See comment above.*

Lines 499-516: Indication of the exact dates when these photos were taken is preferable. *Where known this has been added to figure caption.*

Line 521-532: It would be preferable to indicate and draw lines in each map to show the extents of the remediation and subsequent clean-up operations were executed. *This is included in Figure 11 (now improved), and in discussion.*

Editor's comments:

I have addressed all your comments on style in the revised manuscript.

We have uploaded high resolution images of figures now. Please note that we have improved clarity of many of the figures.

1 **Assessing debris flows using LIDAR differencing: 18th May 2005 Matata event, New**
2 **Zealand.**

3 J. M. Bull^{1#}, H. Miller¹, D.M. Gravley², D. Costello³⁺, D.C.H. Hikuroa³, J.K. Dix¹

4 *^{1#} School of Ocean and Earth Sciences, University of Southampton, National Oceanography*
5 *Centre Southampton, Southampton SO14 3ZH, U.K.*

6 *Email bull@soton.ac.uk*

7 *² Department of Geological Sciences, University of Canterbury, Private Bag 4800,*
8 *Christchurch. N.Z.*

9 *³ School of Environment, The University of Auckland, Private Bag 92019, Auckland, N.Z..*

10 *Corresponding Author*

11 *⁺Now at: Aurecon, PO Box 9762, Newmarket, Auckland, New Zealand, N.Z.*

12 **Keywords:** LIDAR differencing, slope failure, debris flow, sediment pathways, Matata,
13 hazard assessment.

14 *Corresponding Author:*

15 *Jonathan M Bull*

16 *[#] School of Ocean and Earth Sciences, University of Southampton, National Oceanography*
17 *Centre Southampton, Southampton SO14 3ZH, U.K.*

18 *Email bull@soton.ac.uk*

19 **Tel:** 44 (0)2380593078

20

21

22

23

24

25 **ABSTRACT**

26 The town of Matata in the Eastern Bay of Plenty (New Zealand) experienced an extreme
27 rainfall event on the 18th of May 2005. This event triggered widespread landslips and large
28 debris flows in the Awatarariki and Waitepuru catchments behind Matata. LIDAR (Light
29 Detection and Ranging technology) data sets flown prior to and following this event have
30 been differenced and used in conjunction with a detailed field study to identify the
31 distribution of debris and major sediment pathways which, from the Awatarariki catchment,
32 transported at least $350,000 \pm 50,000 \text{ m}^3$ of debris. Debris flows were initially confined to
33 stream valleys and controlled by the density and hydraulic thrust of the currents, before
34 emerging onto the Awatarariki debris fan where a complex system of unconfined sediment
35 pathways developed. Here, large boulders, clasts, logs and entire homes were deposited as the
36 flows decelerated. Downstream from the debris fan, the pre-existing coastal foredune
37 topography played a significant role in deflecting the more dilute currents that in filled
38 lagoonal swale systems in both directions. The differenced LIDAR data has revealed several
39 sectors characterised by significant variation in clast size, thickness and volume of debris as
40 well as areas where post-debris flow cleanup and grading operations have resulted in man-
41 made levees, sediment dumps, scoured channels and substantial graded areas. The application
42 of differenced LIDAR data to a debris flow event demonstrates the techniques potential as a
43 precise and powerful tool for hazard mapping and assessment.

44 **1. Introduction**

45 High-resolution mapping techniques, such as LIDAR (Light Detection and Ranging
46 technology) have the potential to precisely identify and quantify morphological change
47 following a geomorphic event, predict hazard pathways, and map coastal evolution to a high
48 level of accuracy (Revell et al., 2002; Stockdon et al., 2002; Sallenger Jr et al., 2003; White
49 and Wang 2003; Shrestha et al., 2005; Joyce et al., 2009). LIDAR technology has been
50 applied in a number of scientific investigations to rapidly produce detailed topographic
51 models which provide advancements in geomorphological and coastal research (Stockdon et
52 al., 2007). LIDAR is an optical technique that uses the time taken for reflected light to return
53 from objects or surfaces to determine the range, in a similar manner to radar.

54 In this paper, we present an analysis of LIDAR data flown prior to and following a debris
55 flow event at Matata, Bay of Plenty, New Zealand, to identify, map and precisely quantify
56 morphological change. In particular, the study proposes a methodology for LIDAR
57 differencing, and demonstrates this is an effective and valid approach for analysis of
58 sedimentary processes and landscape evolution following a terrestrial slope failure event.

59 Debris flows are a type of terrestrial slope failure or landslide characterised by rapidly
60 moving, water-saturated, non-plastic debris in a steep channel (Hungr, 2005; McSaveney et
61 al., 2005). The principal factors controlling debris flow formation include the duration and
62 intensity of rainfall, the geology and topography of the catchment, rock and soil types,
63 climate, runoff, groundcover and moisture conditions (Manville *et al.*, 2005). This form of
64 slope failure has huge erosive and destructive potential due to its mass, volume, velocity,
65 mobility and run out distance. Debris flows are typically initiated as a landslide on a steep
66 slope before developing into a rapid flow confined by a steep channel, ultimately depositing
67 material downstream on a debris fan (Davies, 2005). The debris fans that develop at the distal

68 end of the depositional zone are often preferred sites for urban development and
69 modification, and they consequently present an increasing hazard to human settlement
70 (Wilford et al., 2004).

71 Geophysical mapping techniques have aided identification of such areas prone to debris
72 flows; however there is only a minor appreciation of the threat posed by such phenomena as a
73 result of the infrequent nature of debris flows within any one stream (McSaveney and Davies,
74 2005). Scientific investigations using LIDAR have highlighted the broad applications of this
75 technology, however there currently is very little research applying this technology for debris
76 flow hazard analysis and morphological change recognition. A recent study that was able to
77 characterise 92% of the lahar (a similar gravity driven flow phenomena to debris flows) path
78 from the 2007 Crater Lake breakout on Mt. Ruapehu in New Zealand revealed that LIDAR is
79 most effective as a mapping and hazard analysis tool when used in combination with other
80 remote sensing data such as satellite imagery (Joyce et al., 2009). The advantage of LIDAR
81 over conventional geodetic techniques is that it can give a synoptic view over a large area.

82 LIDAR data sets flown before and after a debris flow event are compared in this paper, and
83 used for mapping morphological change and for identification of transport and sedimentary
84 processes operating in a dynamic coastal zone. The paper aims to offer one of the first
85 comprehensive assessments of morphological change using LIDAR differencing, to augment
86 understanding of sedimentary transport processes from field and eyewitness accounts, and to
87 more accurately determine the volume of the debris fan deposits and the post event clean-up
88 and rehabilitation measures. These components are important for land-use planning for future
89 hazard mitigation.

90 **2. Regional Geologic Setting**

91 Matata is a small township, located at the coastal fringe in the Eastern Bay of Plenty, in the
92 North Island of New Zealand (Figs. 1 and 2). It sits on the western edge of the Whakatane
93 Graben which is a regional tectonic feature undergoing active extension and forms the
94 northern part (both onshore and offshore) of the Taupo Volcanic Zone (TVZ) (e.g. Beanland
95 et al., 1990; Beanland and Berryman, 1992; Wilson et al., 1995; Rowland and Sibson, 2001;
96 Taylor et al., 2004; Lamarche et al., 2006; Rowland et al., 2009). The TVZ is a rifted
97 volcanic arc (Wilson et al., 1995) that is the product of the coupling between the Pacific and
98 Australian lithospheric plates at the Hikurangi subduction margin off the east coast of the
99 North Island of New Zealand. Rifting in the TVZ is manifest in a series of fault systems, the
100 most active of which is now within the Whakatane Graben. From offshore seismic reflection
101 data, Lamarche et al. (2006) determined a crustal extension rate of 12.6 ± 3.5 mm/yr for the
102 last 20 kyr across the Whakatane Graben. The extension rate decreases to the southwest,
103 along the axis of the TVZ, to < 4 mm/yr at the distal southern end of the zone (Villamor and
104 Berryman, 2006).

105 The coastal zone in this part of the Bay of Plenty region is characterised by inland and coastal
106 sand dunes, as evident at Matata, and also drained peat swamps and flood plains composed of
107 pumiceous alluvium (i.e. the Rangitaiki Plains; Pullar and Selby, 1971; Nairn and Beanland,
108 1989). The town itself is situated between the former wetlands and the steeply rising hills
109 behind, which are composed of mid to late Pleistocene fluvial gravels, marine sediments and
110 interbedded rhyolitic airfall tephra deposits erupted from the TVZ. The stratigraphic sequence
111 is capped by the Matahina ignimbrite, also erupted from the TVZ, which is ~ 300 ka (Bailey
112 and Carr, 1994; Manning, 1996) and extends back into and above the Awatarariki and
113 Waitepuru catchments behind Matata. The Matahina ignimbrite rests directly on
114 marine/beach sediments at a maximum elevation of ~ 250 metres above modern sea level
115 which corresponds to significant uplift (c. < 1 mm yr⁻¹) post c. 300 ka (Gravley et al., in

116 prep). The northern edge of the uplifted block experienced coastal erosion up until c. 7 ka
117 with the remnant coastal cliffs visible today.

118 **3. Eyewitness, Photo and Field Observations of The Matata Debris Flows, 18th**
119 **May 2005**

120 Matata was originally settled on an elevated plateau in front of relatively stable and well-
121 vegetated hills, and has since spread to a less safe and active depositional fan area. On the
122 18th of May 2005, a band of intense rain passed over the hills behind Matata, generating
123 several landslides that coalesced to form two large debris flows within the Awatarariki
124 Stream (catchment area 4.5 km²) and Waitepuru Stream (catchment area 1.3 km²) (Bassett,
125 2006) (Figs. 2 and 3). The closest automatic rain gauge to Matata is about 5 km SSE of
126 Matata (V15: 412 555, near Awakaponga) and on 18th of May 2005 this station recorded a
127 24-hour rainfall of 322 mm. The intensity of the rainfall event is further highlighted by a 1-
128 hour rainfall of 94.5 mm, peaking at 30.5 mm in 15 minutes (McSaveney et al., 2005).
129 Despite little data on past rainfall events of this intensity, 94.5 mm in an hour represents a c.
130 1 in 500 year return period event at this location based on an intensity (rate) that is 30%
131 greater than the 1%-annual-exceedence-probability (see McSaveney *et al.*, 2005 and
132 references therein).The debris flows ultimately emerged from the steep catchments and
133 spread across a fan head at the coastal fringe, destroying 27 homes and transport
134 infrastructure within Matata (Hikuroa et al., 2006).

135 Rapid and recent uplift, combined with the presence of a resistant cap rock (the Matahina
136 ignimbrite) has produced an immature landscape susceptible to debris flows. The Matahina
137 ignimbrite is 20 to 30 metres thick, forms vertical cliffs and has a uniform and relatively
138 impermeable flat-topped surface that protects the underlying, weak to very weak mudstones
139 and siltstones from pervasive erosion (Costello, 2007). From field observations, Costello

140 (2007) modelled a scenario for slope failure whereby the mudstone and siltstones form over-
141 steepened slopes with weathered surfaces that are susceptible to shallow, scallop-shaped
142 slope failures that deliver debris to the stream valleys below. The head scarps from these
143 failures subsequently undermine the overlying ignimbrite, triggering instability and toppling
144 of large slabs of rock. These failure processes are compounded by the presence of
145 unconsolidated sand beds lower in the stratigraphy and close to stream level, allowing for
146 massive undercutting of thick mudstone. The result is massive rock failure and the
147 development of near-vertical and boxed canyon-shaped cliffs with steep debris fans
148 containing up to 100 m³ of boulder to mud-sized grains (Costello, 2007). Together, these
149 slope failures at different levels within the catchment stratigraphy occur on a semi-annual
150 basis and the result is a continuous recharge and supply of boulders, gravels, sand, silt, mud
151 and woody debris to the base of the stream valleys (recharge topple events have been
152 witnessed and recorded by Costello, Gravley and Hikuroa since the May 18 2005 event). The
153 debris then sits perched and ready to be mobilised in the next extreme rainfall event like the
154 one that occurred on May 18 2005.

155 On May 18 2005, the peak rainfall event triggered several landslides within the Awatariki
156 catchment. As described above, these landslides delivered a mixture of boulders, gravels,
157 fines and large woody debris to a rapidly rising stream (McSaveney et al., 2005; Costello,
158 2007). The result was an increase in the mass and volume within the surging current which
159 was then able to mobilise existing and perched ignimbrite boulder beds in the upper
160 catchment and further scour and undermine the channel walls which created fresh debris
161 downstream (Costello, 2007). Based on eyewitness accounts from the landowner adjacent to
162 the stream channel, and oblique aerial photo interpretation (including Fig. 4 and 5), the
163 following sequence of events have been re-constructed. The first surging, debris-laden
164 currents to emerge from the hills passed beneath the railroad bridge and followed an existing

165 stream channel that delivered fresh sediment to the south-eastern lagoon (see Fig. 4). As
166 debris began to pile up behind the rail bridge, it became a sediment barrier that cut off flow
167 into the aforementioned channel and ultimately failed from the back pressure of the
168 subsequent debris flow pulses that were more voluminous and carried the large ignimbrite
169 boulders. Following the failure of the bridge, the debris flows became unconfined, spread out
170 across the pre-existing debris fan, and quickly decelerated which triggered rapid deposition of
171 the heavy boulders and logs (Fig. 5). The rapid loss of mass created a transition from debris
172 to hyperconcentrated flows that carried finer sediment 10's of metres further before it was
173 deposited as smaller lobate fan structures (Fig. 5) and debris floods developed as the currents
174 became even more dilute (Costello, 2007). The debris floods were topographically controlled
175 by the coastal foredunes and followed pathways parallel to the coast, delivering sediment to
176 the lagoon systems (Fig. 6).

177 The spatial distribution of boulders is not uniform over the debris fan: larger boulders of
178 mudstone and ignimbrite are generally deposited on the seaward side of State Highway 2, and
179 a less confined, c. 250 m stretch of the Awatarariki Stream prior to reaching the debris fan.
180 Smaller and less dense boulders of material were transported further and can be found in the
181 distal areas of the fan. Fines and gravels can be found in all areas of the debris fan, and
182 provided the material strength to transport larger boulders. Further evidence of the ability of
183 the flow to transport objects is the presence of large woody debris. Whole-sized trees make
184 up c. 10% of the debris, and were particularly deposited in the lagoon and distal parts of the
185 fan where flow momentum decreased. Anthropogenic debris such as cars, sheds and houses
186 etc are present throughout the debris flow, and some of the larger objects have been
187 transported several hundred metres. While the debris flow deposits from the Waitepuru
188 Stream have a similar lithologic content they lack the abundance of large boulders present in

189 the deposits of the Awatarariki Stream. In this paper, we focus primarily on the depositional
190 fan and associated sedimentation from the Awatarariki debris flows.

191 **4. Methods**

192 This study is based on three high-resolution LIDAR data sets (Fig. 7) which surveyed the
193 coastal zone and wider Rangitaiki Plains in the Bay of Plenty, New Zealand in 2000 and
194 2006. Prior to the Matata debris flow event, a LIDAR data set was collected on the 31st May
195 and 1st June 2000 covering the coastal strip at Matata (Run 5 and 6 - an area of 7.4 km²).
196 After the Matata event, LIDAR data was acquired on the 26th June 2006 specifically over the
197 debris fans. This data images a 3.2 km² swath of ground which covers Matata town and the
198 adjacent coastal and lagoonal environments. Finally, a component (Rang 3 and 4) of the
199 larger Rangitaiki Plains LIDAR data set flown on 14th December 2006 that covers the coastal
200 strip and Rangitaiki Plains adjacent to Matata (an area of 5.2 km²) was used. In the following
201 section we describe analysis of the different data sets, the formation of a single year (pre-
202 debris flow) 2000 data set and a single year (post-debris flow) 2006 data set, and the
203 differencing of the 2006 and 2000 data sets. Begg and Mouslopoulou (2009) describe the
204 complete December 2006 dataset, but do not discuss the Matata debris flow event.

205 The LIDAR data was collected using different systems at different times, and therefore there
206 was an initial stage of pre-processing and inspection of the data to determine the point
207 density/spatial resolution, and comparability. Point density was calculated in areas where the
208 data sets overlapped by analysis of 50 m² bins. This analysis indicated that Krigging of the
209 data onto a 4 m spaced grid was appropriate. In the vast majority of the survey area there
210 were between 2 and 5 data points within each 4 m bin (Miller, 2008).

211 Testing of the vertical accuracy of the LIDAR data can be achieved by comparing RTK (real-
212 time kinematic) terrestrial topography data from the Matata region with the recently acquired

213 LIDAR data (see Miller, 2008 for more details). Due to the sporadic nature of the bench mark
214 sites, only one point is found in a location of both 2000 and 2006 data coverage. The
215 differences between the ground point and LIDAR data in this instance range between +0.34
216 m and +0.4 m. Although this is slightly higher than best-case vertical accuracy estimates for
217 the LIDAR data (± 0.15 m), the difference suggests that the LIDAR datasets are comparable
218 to surface topography data.

219 In order to check on the validity of combining the different gridded LIDAR data sets, a
220 comparison of the vertical height differences was made between the different data sets (Fig.
221 7) in areas of overlap away from man-made features, where topography was relatively
222 subdued, and away from the dynamic coastal fringe. We examined areas of overlap between
223 Run 5 and Run 6 for the 2000 LIDAR data. For the 2006 data, Rang 3 and Matata, Rang 4
224 and Matata and the overlap between Rang 3 and Rang 4 were analysed.

225 From the vertical difference of the selected area, an error range was selected to represent the
226 mean differenced value ± 1 standard deviation (Table 1). The largest error range is calculated
227 to be ± 0.2 m (Table 1), which means that when differencing the LIDAR data sets elevation
228 changes less than ± 0.4 m are meaningless.

229 Following vertical accuracy testing of the data, the two separate runs from the 2000 data (Run
230 5 and 6) were combined. A composite file was also produced for the 2006 data using the
231 Matata, Rang 3 and Rang 4 data sets. The two composite rasters (gridded at 4 m) were
232 differenced and the output image interpreted. Drawing upon the results above, data values
233 which fell within the defined error range of ± 0.4 m were excluded.

234 Georeferenced aerial photography provided a high-resolution collection of images covering
235 Matata town, the coastal zone and the wider Rangitaiki Plains, which helped validate the

236 findings of the LIDAR data, and enabled further insights into the terrain, sedimentary
237 processes and hazard assessment.

238 **5. Results**

239 The topographic maps using the LIDAR data record the land surface pre- and post-event (Fig.
240 8). The spatial extent of these maps range from the base of the steeply rising hills located
241 behind Matata to the coastal and dune system. This region fully covers the area where the
242 Awatarariki Stream channel loses confinement and also maps the township of Matata and the
243 surrounding coastal flats and lagoon environment. The more recent 2006 LIDAR data set also
244 includes data mapping the Awatarariki Stream and catchment, which extends into the hills
245 behind Matata.

246 The quality of the pre-event LIDAR data is reduced in comparison with the 2006 data set, the
247 latter having higher point density and greater vertical accuracy and horizontal resolution. This
248 accounts for the sporadic data gaps in the 2000 topography (Fig. 8). Despite this, change in
249 topography over the intervening period is clearly visible, and areas where previous low
250 elevation has preferentially increased in height are identifiable. The changes in topography
251 show a general increase in elevation across the coastal flats, with up to 2 m of height increase
252 in certain locations. This sediment deposition is in the form of a fan, the apex of which is at
253 the point where the Awatarariki Stream loses confinement (i.e. the drainage point of the
254 Awatarariki Stream catchment). The topographic data further illustrates that a more defined
255 channel flowing into the lagoon has developed in the intervening period between 2000 and
256 2006 (Fig. 8). This channel is characterised by flanking levee deposits of increased elevation
257 (see later discussion for the origins of this change). In addition, the lagoon environment
258 which this channel flows into is also well defined by the LIDAR data.

259 The LIDAR data in the topographic plots is used primarily to examine the key region of
260 interest, and has demonstrated significant change in topography following the Matata debris
261 flows. This can be further assessed and built upon through comparison with the differenced
262 plots, which precisely map the distribution of morphological change following the debris
263 flow event in 2005. These plots illustrate quantifiable areas of erosion and deposition in the
264 form of sedimentary features and geomorphic landforms associated with the Awatarariki
265 Stream course. Erosion scarps and pockets of deposition are captured in the differenced
266 image along the coastal hill slopes west of Awatarariki catchment (Fig. 9a, area A).

267 The Awatarariki Stream, which conveyed a large proportion of the debris flow, can be
268 identified in the differenced plot as an s-shaped channel traversing the coastal flats from west
269 to east and connecting with the lagoonal depositional environment (Figs. 9a and b, Line B-
270 B'). There is evidence for 1 – 2 m removal of material at the channel bed and a further
271 removal of up to 2 m to the east of the channel (Figs. 9a and b, areas C and D respectively).
272 Elongated levee deposits flank this channel and are approximately 10 m in width (although
273 this is variable and can be as wide as 20 m) and have a mean height of around 1 m, with a
274 maximum height of 4.5 m (Fig. 9b, Line B-B'). These mapped changes in elevation are
275 comparable to the findings of the topographic plots.

276 Deposition of material on the coastal flats in the vicinity of Matata is in the general form of a
277 fan, with sediment deposition taking place at the point where the Awatarariki Stream loses
278 confinement (Fig. 9a, Point E). We define the main depositional fan as the area between the
279 point of flow expansion (Point E) and the lobate fan structures (J-J'; Figs 5 and 10), where
280 the transition between debris flows/hyperconcentrated flows and debris floods occurs (see
281 Section 3)

282 Both the topographic plots and the differenced data show that at point E, there is an increase
283 in depositional area due to lateral flow expansion and material expelled onto the debris fan in
284 a process which built topography. The same data clearly shows, beyond the debris fan,
285 infilling of topography that parallels the coastline to the northwest (where a wetland existed,
286 Fig. 2., prior to the flow event) and to the southeast towards the lagoon (Fig. 10). Another
287 factor characterising fan development is the presence of irregular fingers of higher elevation
288 (Fig. 9, area F). At the margins of the debris fan is an anomalously large, oval shaped deposit
289 approximately 200 m in length, 50 m in width and of a maximum height of 11 m (Fig. 9a,
290 area G).

291 The lagoonal system is characterised by patchy data coverage because the water prevents
292 consistent reflected LIDAR returns and no elevation can be calculated. However where
293 water depth is particularly shallow then some elevation data (e.g. bathymetry) could be
294 obtained. Despite these issues, there are a number of data points which map elevation in the
295 western lagoon section which show that there is a net increase in residual silt levels following
296 the debris flow and subsequent debris flood. The differenced plot suggests the silt level
297 equals, and in places is up to 0.7 m higher than the original bathymetric level (Fig. 9b, area
298 H). The difference plots delineate the lateral extent of deposition within the lagoon (Fig. 9b,
299 area I). This coincides with the presence of a causeway which bisects the lagoon and appears
300 to have effectively acted as a barrier to the spread of debris further to the east.

301 **6. Discussion**

302 The LIDAR data has successfully identified, mapped and precisely quantified morphological
303 change following the terrestrial slope failure event at Matata. The differenced data identified
304 the location of sediment deposition and erosion and has been used to confirm the sediment
305 transport and deposition processes described by eye witnesses and subsequent field

306 observation. However it is important to recognise that the differenced data delineates
307 landscape change due to both the debris flow and flood, but also the subsequent clean-up
308 operations. The post-event clear up operations are best shown by the oval-shaped sediment
309 deposit (area G, Fig. 9a), which is the largest positive elevation in the differenced plot in an
310 area of previously low topography and was the site where material was moved to and dumped
311 during clean-up operations. Additional anthropogenic modification detected in the LIDAR
312 data include the build up of levees (B-B', Figs. 9a and b) from material (up to 2 m deep)
313 excavated from the stream channel floor (Fig. 9a, area C). These levees have been
314 constructed to augment a confined flow path within the excavated channel and, thus,
315 constitute the surface morphology visible today. These examples of post-event modification
316 of morphology demonstrate LIDAR differencing can be a valid and effective tool to identify
317 mass movement and precise changes in the landscape over a small area. However, LIDAR
318 cannot be used in isolation and complementary field studies are required to validate
319 anthropogenic modification. Furthermore, it is desirable that LIDAR data should be flown
320 immediately following an event (i.e. before clean-up operations) if the natural landscape-
321 modifying processes are to be fully understood.

322 Eyewitness and field observations were used to determine the spatial variations in flow
323 processes (Section 3), but the differenced plot (Fig. 9a) clearly detects mini finger-like levee
324 structures on top of the debris fan (from point E to Line J-J') and the lobate boulder train
325 deposit at the edge of the fan. This arcuate-shaped feature in the differenced LIDAR data
326 marks the point at which the boulder front stalled and the more dilute material from the main
327 body of the flow broke through (Hung, 2005), developing smaller subsequent fans and
328 feeding an area of low topography to the northwest (the elongate wetlands seen in the coastal
329 strip northwest of the Awatarariki debris fan in Fig. 2). Comparison of topographic maps
330 (Fig. 8) of the land surface pre- and post-event reveal that this area, of previous low

331 elevation, preferentially increased in height due to deposition of material that was transported
332 along identifiable pathways controlled by pre-existing topography (Fig. 10). This is the most
333 obvious example of topography-driven flow.

334 The topographic and differenced LIDAR data further identify a sediment pathway to the
335 southeast (Fig. 10), where a proportion of material was transported to the lagoon system via a
336 pre-existing channel. The presence of debris including large trees at the exit of this channel in
337 the lagoon (Fig. 9b, area H) suggests that to begin with, this channel provided a conduit to the
338 lagoon. It can be inferred that this channel was infilled relatively quickly following the
339 initiation of the debris flow event, given the volume of material and the clast rich and boulder
340 bearing surges which characterised the event. Hard to very hard (welded) ignimbrite boulders
341 from the Matahina formation and weak siltstone and silty sandstone boulders which originate
342 from the Pleistocene marine sediments found in the catchments behind Matata are the source
343 of these clast rich and boulder-bearing surges (McSaveney et al., 2005). Eye witness studies
344 suggest that the channel was subsequently bypassed after the rail bridge initially trapped
345 material, and then failed allowing the debris fan to become unconfined (Fig. 10).

346 The differenced LIDAR data can be used for precise quantification of morphological change
347 following the terrestrial slope failure event at Matata but it has some limitations. The raised
348 foredune system prevented loss of material to the sea, however a substantial amount of
349 material entered into the lagoon system, and this material was not fully detectable by the
350 LIDAR differencing due to the water layer absorbing the light. Recently collected core data
351 acquired within the lagoon as part of Matata Regeneration works by Tonkin and Taylor Ltd,
352 found that between 0.4 and 1.8 m of debris from the 2005 event was deposited in the lagoon
353 with an average thickness of 1.0 m. Our approach is to use the differenced LIDAR data to
354 calculate the volume of the debris flow outside of the lagoon, and the core data to calculate
355 the amount deposited within the lagoon. These volumes can then be compared to the

356 estimates of Costello (2007) who used field surveying to estimate the amount of material
357 outside of the lagoon.

358 In our calculations we divide the area of deposition into the main debris fan and the area of
359 the debris flood to the northwest of the fan. We add in the material moved as part of the
360 clean-up operation into our estimate where this was easily identified. Table 2 summarises the
361 total volumes calculated from the field observations, and from the LIDAR data. For the areas
362 outside of the lagoon we find 300,000 m³ derived from field observations, and 260,000 m³
363 from the LIDAR differencing. Errors on these estimates are large, perhaps $\pm 50,000$ m³, and
364 therefore the estimates from the two different approaches are broadly consistent. Any
365 systematic difference is most likely to be due to difficulties in estimating the thickness of
366 deposits in areas of low lying relief in the field observations.

367 The 27 boreholes acquired were concentrated within the centre of the lagoon system, and
368 therefore we do not have good control on deposition at the margins of this area which were
369 flooded during the event. Taking a conservative approach we find that a minimum of 90,000
370 m³ was deposited within the lagoon, beyond the detection limits of the LIDAR data (under
371 water). We therefore find a total debris flow volume of $390,000 \pm 50,000$ m³ estimated by
372 field observations and $350,000 \pm 50,000$ m³ estimated by the LIDAR data. These figures are
373 both substantially higher than the estimate made by rapid reconnaissance immediately after
374 the debris flow of c. 250,000 m³ (McSaveney et al., 2005). The major reasons for this
375 discrepancy are likely to be underestimates of the material deposited by the debris flood in
376 areas of originally low topography.

377 These findings demonstrate the capabilities and huge potential of LIDAR to precisely
378 quantify change following a mass movement event, and build upon field observations to
379 calculate volumetric change. Such accurate measurements of morphological change are vital

380 in precise hazard assessment studies. In particular, accurate calculations for the volume of
381 debris that came from the Awatarariki catchment during the 2005 event are essential to
382 making future land-use planning decisions and mitigating damage to infrastructure and
383 lifelines (i.e. rail and road bridges) through appropriate engineering and design. The
384 frequency of debris flows emanating from Awatarariki catchment is poorly understood, but
385 what is known is that the catchment has been destabilised and landslips continue to deliver
386 fresh sediment to the valley floor today. As a consequence, the triggering of a future debris
387 flow event of a similar magnitude may not require a 500-year rainfall event. If and/or when
388 the next debris flow event occurs, it is clear that LIDAR could be used to accurately assess
389 volumetric change and significantly aid clean-up operations.

390

391 **7. Conclusions**

392 A terrestrial slope failure event in New Zealand has been successfully mapped and
393 investigated using a LIDAR differencing technique. This investigation confirms the
394 capabilities and validity of using high-resolution differenced LIDAR data sets as a
395 geophysical mapping tool for coastal science and mass movement assessments. LIDAR
396 differencing permits precise quantification and accurate mapping of a dynamic environment
397 following a terrestrial slope failure event, and is useful for hazard assessment.

398 The LIDAR differencing technique estimated a minimum volume of $350,000 \pm 50,000 \text{ m}^3$ for
399 the debris flows which is comparable to estimates from detailed field observations $390,000 \pm$
400 $100,000 \text{ m}^3$. The LIDAR data gives a comprehensive overview of the deposit, and identified
401 volumes deposited by both the debris flow, but also the debris flood. The infilling of pre-
402 existing low topography by the debris flood was notable in the Matata event.

403 While LIDAR differencing can be successfully used to study landscape evolution and make
404 volumetric estimates of change, it is important that the post-event survey occurs immediately
405 following the event, and before any major site remediation has taken place.

406 **Acknowledgements**

407 We are grateful to Environment Bay of Plenty Regional Council, New Zealand, for provision
408 of the LIDAR and terrestrial topography data, and thank Peter West and Mark Langridge for
409 their assistance. Helen Miller was supported by the University of Southampton (Richard
410 Newitt Bursary) and the Society for Underwater Technology (Educational Support Fund).
411 Without the ground support of Anthony Olsen and the Matata Community Centre, the field
412 work would not have been possible. In addition, the eyewitness accounts provided by Neville
413 Harris were invaluable to this research. We thank David Bouma of Tonkin and Taylor Ltd for
414 making available core information within the lagoon. We thank Colin Wilson, Julie Rowland
415 and Pierre Cazenave for their support.

416 **References**

- 417 Bailey, R.A., Carr, R.G., 1994. Physical volcanology and eruptive history of the Matahina
418 Ignimbrite, Taupo Volcanic Zone, New Zealand. *N. Z. J. Geol. Geophys.* 37, 319-344.
- 419 Bassett, T, 2006. The Matata debris flows, 18 May 2005. *Monitoring, Simulation, Prevention*
420 *and Remediation of Dense and Debris Flows.* WIT Trans. Ecol. Envir. 90, 363-370.
- 421 Beanland, S., Blick, G. H., Darby, D. J., 1990. Normal faulting in a back arc basin: geological
422 and geodetic characteristics of the 1987 Edgecumbe earthquake, New Zealand. *J. Geophys.*
423 *Res.* 95, 4693-4707.
- 424 Beanland, S., Berryman, K. R., 1992. Holocene coastal evolution in a continental rift setting;
425 Bay of Plenty, New Zealand. *Quatern. Int.* 15/16, 151-158.

426 Begg, J. G., Mouslopoulou, V., 2009. Analysis of late Holocene faulting within active rift
427 using lidar, Taupo Rift, New Zealand. *J. Volcanol. Geotherm. Res.* 190, 152-167.

428 Costello, D.A., 2007. Slope failures and debris flow assessment at Matata, Bay of Plenty,
429 New Zealand. Masters Thesis, Univ. Auckland, New Zealand.

430 Davies, T., 2005. Debris flow emergency at Matata, New Zealand, 2005. Inevitable events,
431 predictable disaster. Internal Report Natural Hazards Research Centre, Department of
432 Geological Sciences, Univ. Canterbury, New Zealand.

433 Hikuroa, D.C.H., Gravley, D.M., Wilson, C.J.N., Browne, P.R.L., Olsen, A.W., 2006. Recent
434 stratigraphic studies at Matata: implications for Kawerau geothermal field modelling and
435 subsurface interpretation. Proceedings, 28th New Zealand Geothermal Workshop.

436 Hungr, O., 2005. Classification and terminology. In: Jakob, M. and Hungr, O., (Eds.) Debris-
437 flow hazards and related phenomena, Springer and Praxis Publishing, pp. 9-23.

438 Joyce, K.E., Samsonov, S., Manville, V., Jongens, R., Graettinger, A., Cronin, S.J., 2009.
439 Remote sensing data types and techniques for lahar path detection: A case study at Mt.
440 Ruapehu, New Zealand. *Remote Sens. Environ.* 113, 1778-1786.

441 Lamarche, G., Barnes, P. M., Bull, J. M., 2006. Faulting and extension rate over the last
442 20,000 years in the offshore Whakatane Graben, New Zealand continental shelf. *Tectonics*
443 25(TC4005): 1-24.

444 Manning, D.A., 1996. Middle-late Pleistocene tephrostratigraphy of the eastern Bay of
445 Plenty, New Zealand. *Quatern. Int.* 34-36, 3-12.

446 Manville, V., Newton, E. H., White, J. D. L., 2005. Fluvial responses to volcanism:
447 re-sedimentation of the 1800a Taupo ignimbrite eruption in the Rangitaiki River catchment,
448 North Island, New Zealand. *Geomorphology* 65, 49-70.

449 McSaveney, M. J., Beetham, R. D., Leonard, G. S., 2005. The 18 May 2005 debris flow
450 disaster at Matata: causes and mitigation suggestions. *Institute of Geological & Nuclear*
451 *Sciences*, Client Report 2005/71, 1-50.

452 McSaveney, M. J., Davies, T. R. H., 2005. Engineering for debris flows in New Zealand. In:
453 Jakob, M. and Hungr, O., (Eds.) *Debris-flow hazards and related phenomena*, Springer and
454 Praxis Publishing, pp. 635-657.

455 Miller, H., 2008. Examination of terrestrial slope failures, sedimentary processes and coastal
456 evolution using LIDAR data around Matata, Bay of Plenty, New Zealand. MSc Thesis. Univ.
457 Southampton, U.K., 65p

458 Nairn, I. A., Beanland, S., 1989. Geological setting of the 1987 Edgecumbe earthquake, New
459 Zealand. *N. Z. J. Geol. Geophys.* 32, 1-13.

460 Pullar, W. A., Selby, M. J., 1971. Coastal progradation of Rangitaiki Plains, New Zealand.
461 *N.Z. J. Sci.* 14, 419-434.

462 Revell, D. L., Komar, P. D., Sallenger Jr, A. H., 2002. An application of LIDAR to analyses
463 of El Niño erosion in the Netarts littoral Cell, Oregon. *J. Coastal Res.* 18, 792-801.

464 Rowland, J. V., Sibson, R. H., 2001. Extensional fault kinematics within the Taupo Volcanic
465 Zone, New Zealand: soft-linked segmentation of a continental rift system. *N. Z. J. Geol.*
466 *Geophys.* 44, 271-283.

467 Rowland, J. V., Wilson, C. J. N., Gravley, D. M., 2009. Spatial and temporal variations in
468 magma-assisted rifting, Taupo Volcanic Zone, New Zealand. *J. Volcanol. Geotherm. Res.*
469 190, 89-108.

470 Sallenger Jr, A. H., Krabill, W. B., Swift, R. N., Brock, J., List, J., Hansen, M., Holman, R.
471 A., Manizade, S., Sontag, J., Meredith, A., Morgan, K., Yunkel, J. K., Frederick, E. B.,
472 Stockdon, H., 2003. Evaluation of airborne topographic lidar for quantifying beach changes.
473 *J. Coastal Res.* 19, 125-133.

474 Shrestha, R. L., Carter, W. E., Sartori, M., Luzum, B. J., Slatton, K. C., 2005. Airborne laser
475 swath mapping: quantifying changes in sandy beaches over time scales of weeks to years. *J.*
476 *Photogram. Rem. Sens.* 59, 222-232.

477 Stockdon, H. F., Sallenger Jr, A. H., List, J. H., Holman, R. A., 2002. Estimation of shoreline
478 position and change using airborne topographic lidar data. *J. Coastal Res.* 18, 502-513.

479 Stockdon, H. F., Lillycrop, W. J., Howd, P. A., Wozencraft, J. M., 2007. The need for
480 sustained and integrated high-resolution mapping of dynamic coastal environments. *Mar.*
481 *Technol. Soc. J.* 40, 90-99.

482 Taylor, S.K., Bull, J.M., Lamarche, G., Barnes, P.M., 2004 Normal fault growth and linkage
483 during the last 1.3 million years: an example from the Whakatane Graben, New Zealand. *J.*
484 *Geophys. Res.* 109, B02408, doi:10.1029/2003JB002412.

485 Villamor, P., Berryman, K.R., 2006. Late Quaternary geometry and kinematics of faults
486 at the southern termination of the Taupo Volcanic Zone, New Zealand. *N. Z. J. Geol.*
487 *Geophys.* 49, 1-21.

488 White, S. A., Wang, Y. W., 2003. Utilizing DEMs derived from LIDAR data to analyse
489 morphologic change in the North Carolina coastline. *Remote Sens. Environ.* 85, 39-47.

490 Wilford, D. J., Sakals, M. E., Innes, J. L., Sidle, R. C., Bergerud., W. A., 2004. Recognition
491 of debris flow, debris flood and flood hazard through watershed morphometrics. *Landslides*
492 1, 61-66.

493 Wilson, C. J. N., Houghton, B. F., McWilliams, M. O., Lanphere, M. A., Weaver, S. D.,
494 Briggs, R. M., 1995. Volcanic and structural evolution of Taupo Volcanic Zone, New
495 Zealand: a review. *J. Volcanol. Geotherm. Res.* 68, 1-28.

496 **Figure Captions**

497 **Fig. 1.** Regional setting of Matata on the northern edge of the Taupo Volcanic Zone (TVZ),
498 New Zealand. Major rivers are indicated draining northward into the Bay of Plenty.

499 **Fig. 2.** Aerial photo (260-V15) showing location of Awatarariki and Waitepuru catchments
500 behind the coastal cliffs around Matata, Bay of Plenty, New Zealand. These catchments
501 produced the damaging 18th May 2005 Matata debris flows. The image was taken prior to the
502 debris flow and shows wetlands in the coastal strip west of the Awatarariki Stream which
503 were covered by the debris flow.

504 **Fig. 3.** 3D perspective of Awatarariki and Waitepuru catchments created using a 5 m DEM
505 from LINZ 1:50,000 contours, and spot heights. The position of Matata and the coastal
506 corridor seaward of the palaeo-cliffs are indicated.

507 **Fig. 4.** Aerial Photograph (courtesy Terrain Consultants) showing in detail where the debris
508 flow emerged from the confinement of the Awatarariki Stream. The first debris-laden
509 currents passed beneath the railroad bridge and followed an existing stream channel
510 (indicated by the white dotted line). After debris build-up behind the bridge and its failure,

511 the main debris flow bypassed the channel and spread out in an unconfined way across the
512 pre-existing fan with huge truck-sized boulders visible in the proximal fan. Remediation
513 efforts had just commenced when this photograph was taken.

514 **Fig. 5.** Aerial photograph (courtesy Whakatane Beacon, taken 18th May 2005) showing the
515 debris flow from the Awatarariki Stream. The emergence of the Awatarariki Stream onto the
516 flat coastal plain is visible, as is the lobate boulder train. This photograph was taken before
517 any remediation activity and is a good record of the immediate aftermath of the debris flow.
518 Large boulders were limited to the area between the line of the buildings and the base of the
519 hill. Fine debris was deposited as a debris flood in the foreground, while the dashed white
520 lines indicate small lobate fan structures.

521 **Fig. 6.** Oblique aerial photograph (courtesy Whakatane Beacon, taken 18th May 2005),
522 looking southwest, showing debris entering the western portion of the Matata lagoon, and
523 associated silt-laden waters. Much of the fine sediment was not confined to the fan from the
524 Awatarariki Stream, but was carried into the lagoon.

525 **Fig. 7.** Location of LIDAR data files – Run 5, Run 6, Matata, Rang 3 and Rang 4. Aerial
526 photographs for context were flown in March 1987 by New Zealand Aerial Mapping Ltd.
527 Areas of overlap used for analysis in producing the integrated pre-debris flow (2000) and
528 post-debris flow (2006) topography are indicated.

529 **Fig. 8.** Composite figure of a selected area affected by the debris flow. **A:** 2000 topography
530 **B:** 2006 topography. All contours at 1 m intervals.

531 **Fig. 9.** Difference in vertical height between the 2000 and 2006 LIDAR data (a) for an area
532 including the Awatarariki stream and (b) an area to the east including Matata lagoon
533 (locations shown in Fig. 2). Contours are at 1 m intervals. Lettered areas are referred to in

534 main text. Classification of heights around the mean has resulted in high values assigned no
535 colour, as at area G. In this location, the maximum height is 11 m.

536 **Fig. 10.** Sediment pathways map, showing deposition following the 2005 Matata debris flow
537 event. Arrows show the sediment transport pathways. Line J – J' is discussed in the main
538 text.

539

540

541

542

543

544

545

546

547

548

549

550

551

552

553 **Table 1.** Vertical height comparison in areas of data overlap (Fig. 7). The range of vertical
 554 height difference of clipped areas is biased by the inclusion of outliers, and therefore a better
 555 measure of the differences is the mean \pm 1 standard deviation.

556

557

Year flown	Data sets compared in overlap area	Range of vertical height differences (m)	Error range (m) Mean \pm 1 Stdev	Overall max error range
2000	Run 5 + Run 6	-1.44 – 0.76	-0.07 \pm 0.18	\pm 0.4 m
2006	Rang 3 + Matata	-0.31 – 1.00	0.18 \pm 0.125	
	Rang 4 + Matata	-0.87 – 0.86	0.1 \pm 0.16	
	Rang 3 + Rang 4	-0.02 – 0.20	0.1 \pm 0.1	

558

559

560

561

562

563

564

Field Observations	Location	Volume (m³)
	Main Debris Fan	110,000
	Debris Flood (to the north-west)	190,000
	Total Field	300,000
LIDAR Differenced data		
	Main Debris Fan	120,000
	Debris Flood (to the north-west)	80,000
	Material moved before LIDAR acquired	60,000
	Total LIDAR	260,000
Sediment Cores in Lagoon		
	Sediment deposited in lagoon (Minimum)	90,000
Total LIDAR-based (Minimum)	Field observations + Lagoon	390,000
Total Field-based (Minimum)	LIDAR + Lagoon	350,000

565 **Table 2.** Estimates of volume of debris flow produced by Awatariki Catchment in Matata
566 2005 debris flow calculated from field observations (Costello, 2007) and using LIDAR
567 differencing (this paper), and using thicknesses of 27 sediment cores within the lagoon. Some
568 of differences between seen in estimates of Debris Fan and Debris Flood deposits between
569 the field observations and LIDAR data, could be due to clean-up prior to the second LIDAR
570 flight. Where known, the volume of material removed (e.g. to location G, Fig 9a) has been
571 incorporated in the estimates.

Figure1
[Click here to download high resolution image](#)

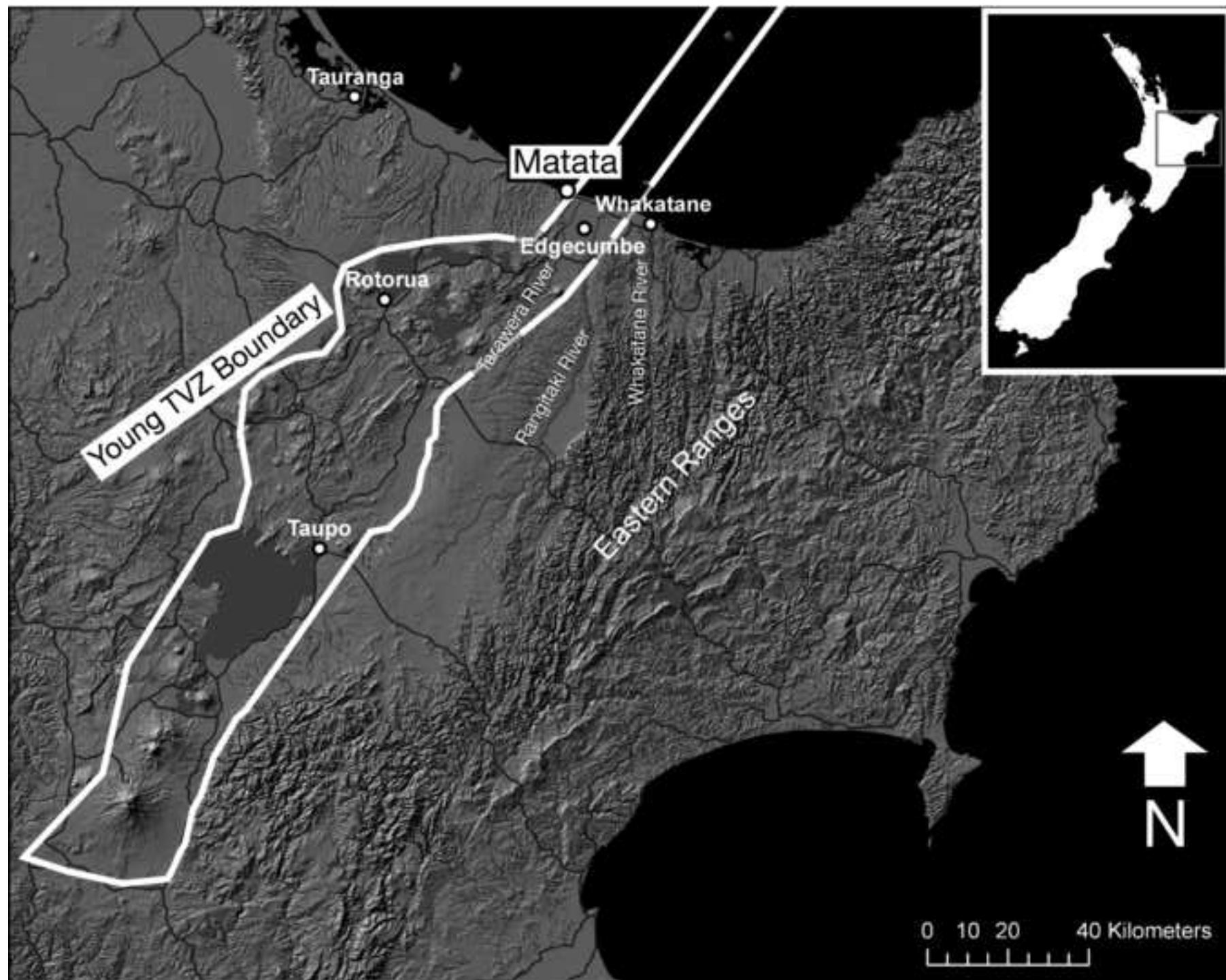


Figure2

[Click here to download high resolution image](#)

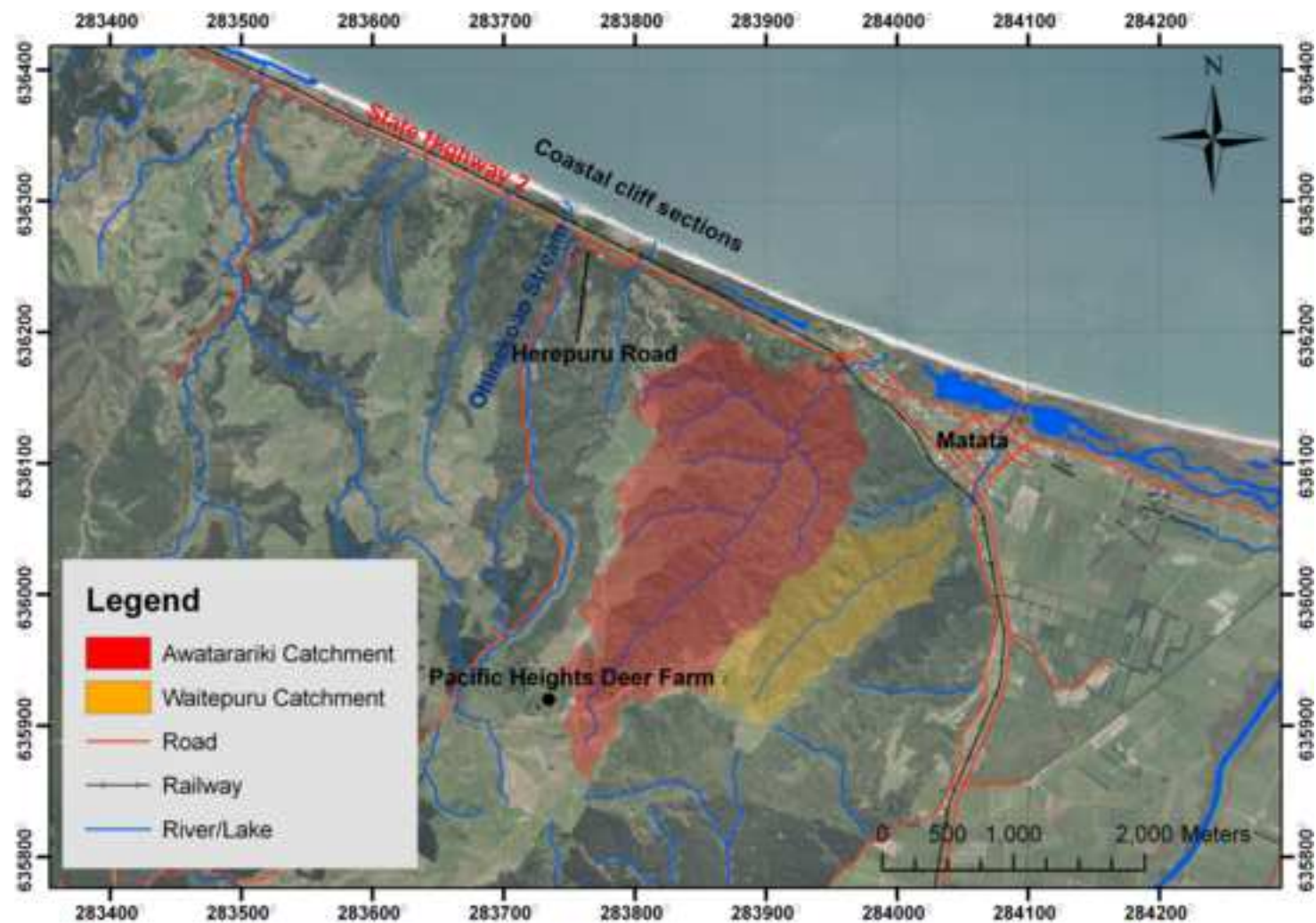


Fig. 2. Aerial photo showing location of Awatarariki and Waitepuru catchments behind the coastal cliffs around Matata, Bay of Plenty, New Zealand. These catchments produced the damaging 18th May 2005 Matata debris flow. The image was taken prior to the debris flow and shows wetlands in the coastal strip west of the Awatarariki Stream which were covered by the debris flow.

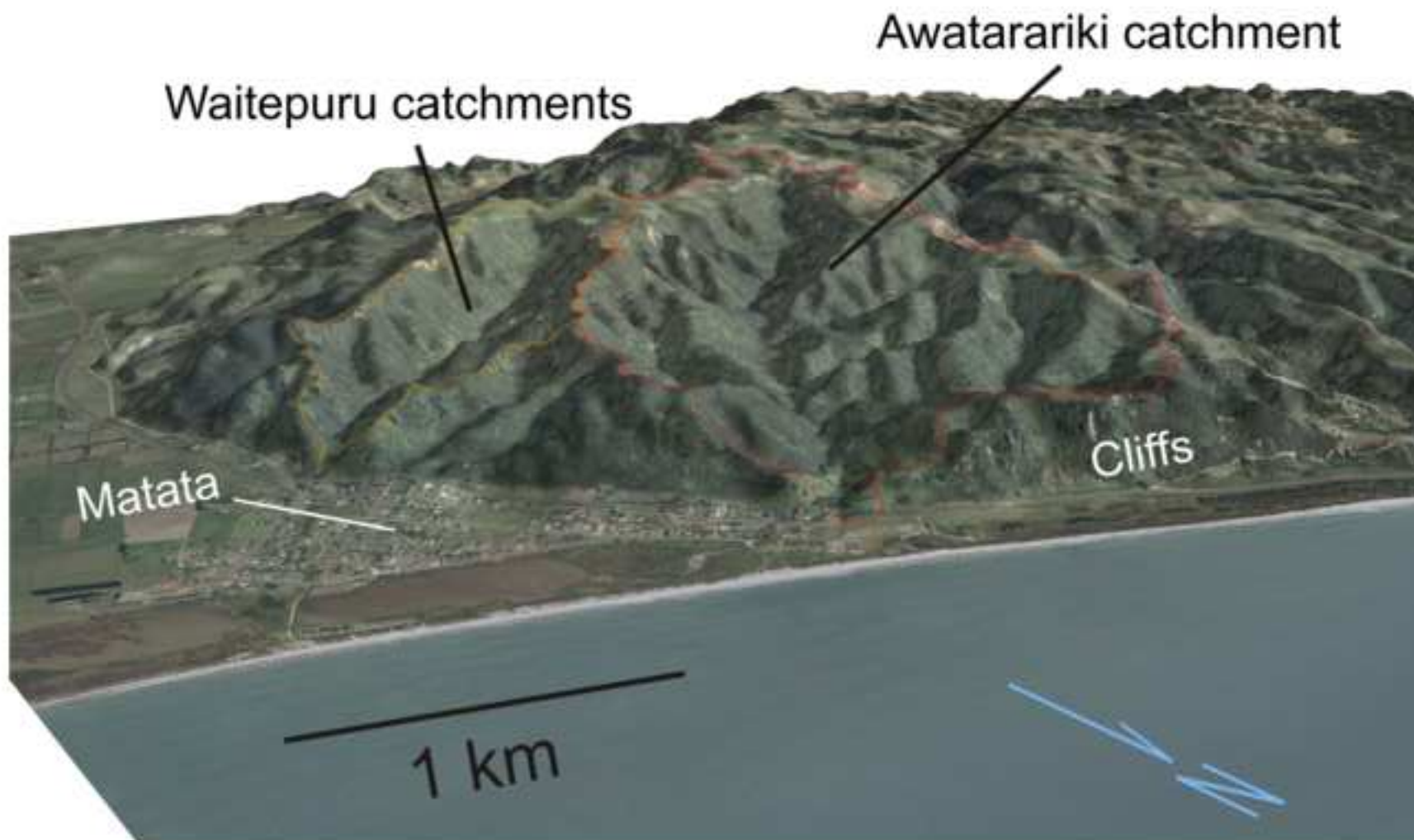


Fig. 3. 3D perspective of Awatarariki (red) and Waitepuru (yellow) catchments created using a 5 m DEM from LINZ 1:50,000 contours, and spot heights. The position of Matata and the coastal corridor seaward of the paleo-cliffs are indicated.

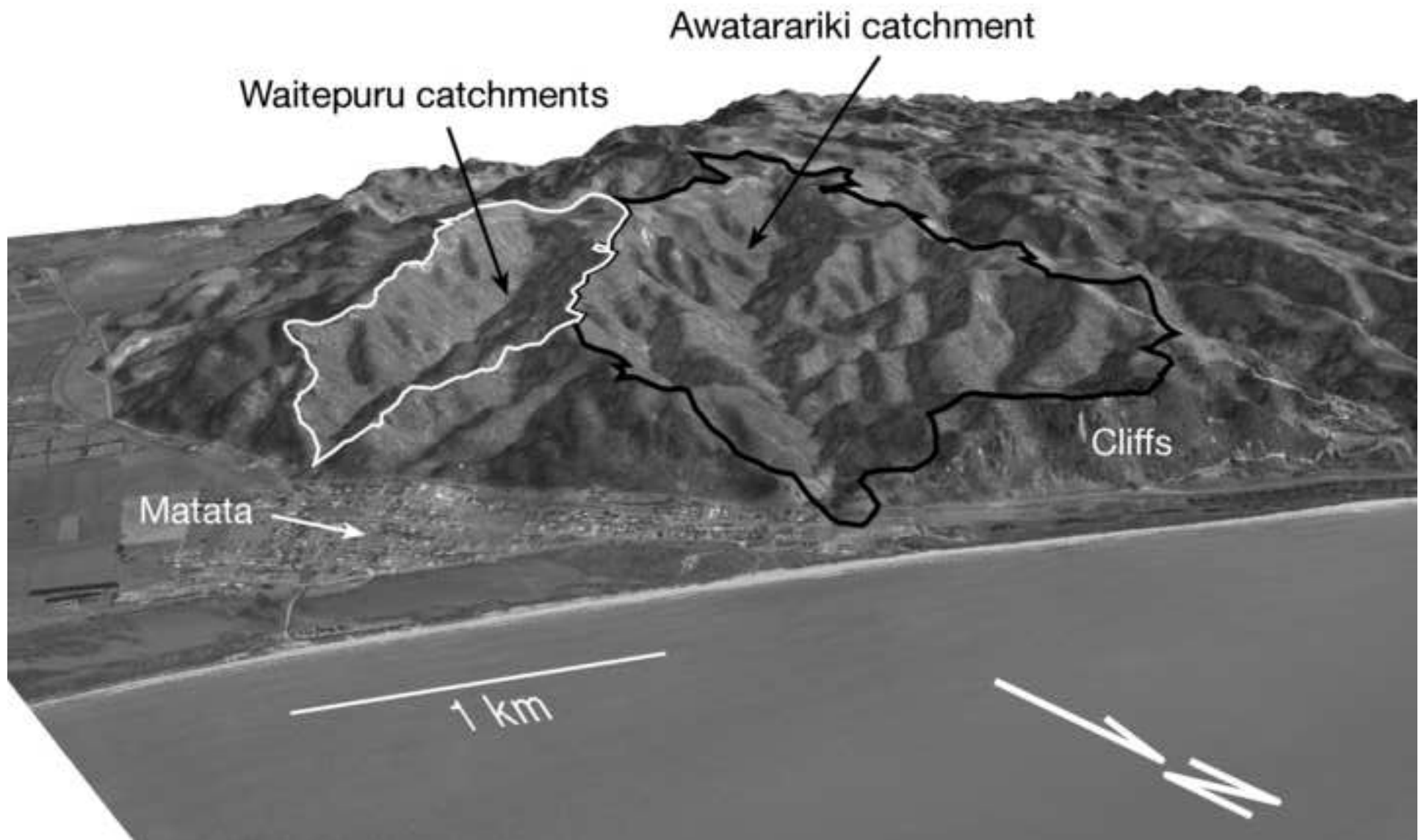




Fig. 4. Aerial Photograph (courtesy Terrain Consultants) showing in detail where the debris flow emerged from the confinement of the Awatarariki Stream. The first debris-laden currents passed beneath the railroad bridge and followed an existing stream channel (white dotted line). After debris build-up behind the bridge and its failure, the main debris flow bypassed the channel and spread out in an unconfined way across the pre-existing fan with large truck-sized boulders visible in the proximal fan. Remediation efforts had just commenced when this photograph was taken.



Fig. 5. Aerial photograph (courtesy Whakatane Beacon) showing the debris flow from the Awataraniki Stream. The emergence of the Awataraniki Stream onto the flat coastal plain is visible, as is the lobate boulder train. This photograph was taken before any remediation activity and is a good record of the immediate aftermath of the debris flow. Large boulders were limited to the area between the line of the buildings and the base of the hill. Fine debris was deposited as a debris flood in the foreground, while the dashed white lines show small lobate fan structures.

Figure6

[Click here to download high resolution image](#)



Fig. 6. Oblique aerial photograph (courtesy Whakatane Beacon), looking southwest, showing debris entering the western portion of the Matata lagoon, and associated silt-laden waters. Much of the fine sediment was not confined to the fin from the Awatanuki Stream, but was carried in the lagoon.

Figure7_colour
[Click here to download high resolution image](#)

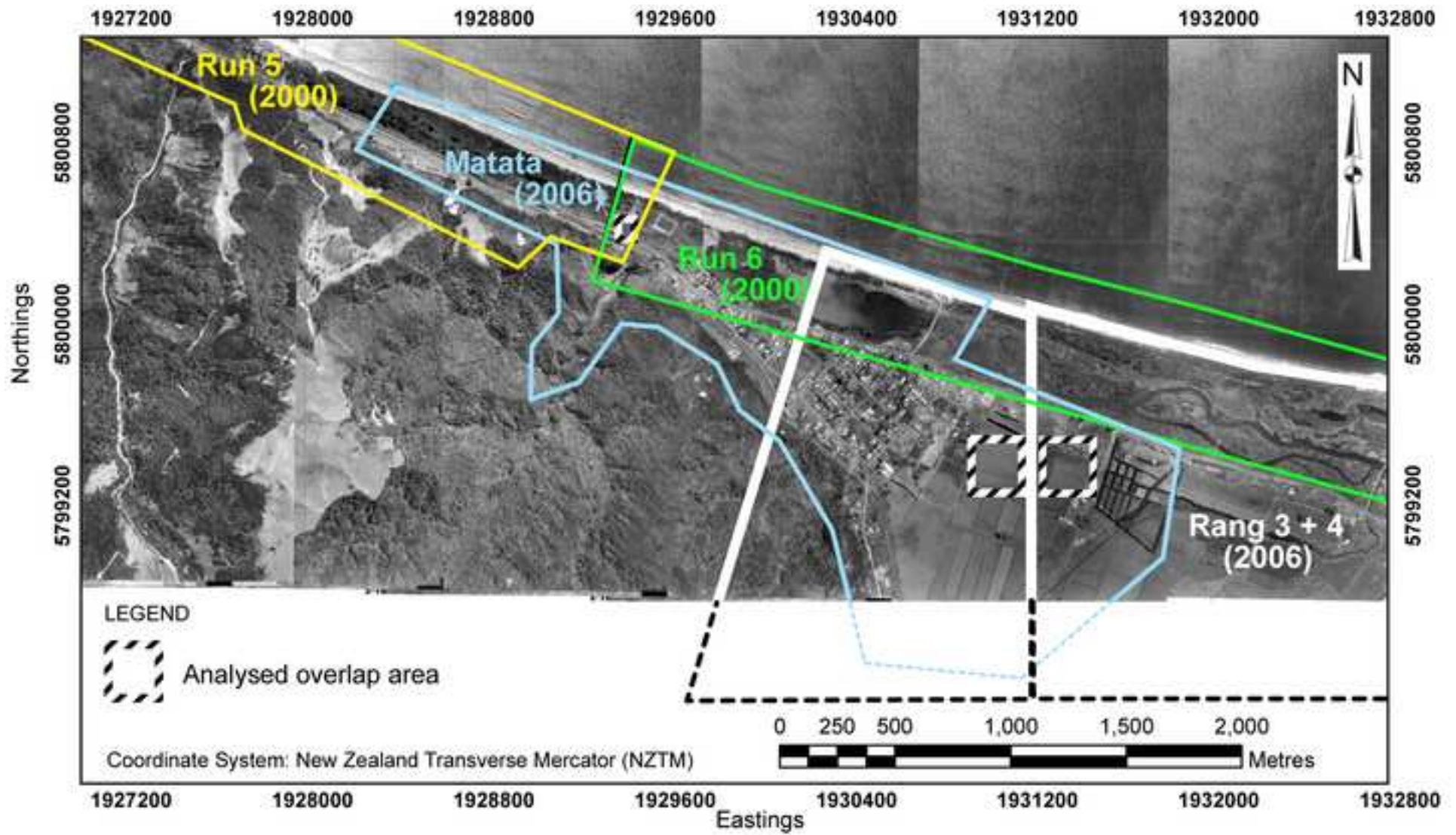


Figure7_bw
[Click here to download high resolution image](#)

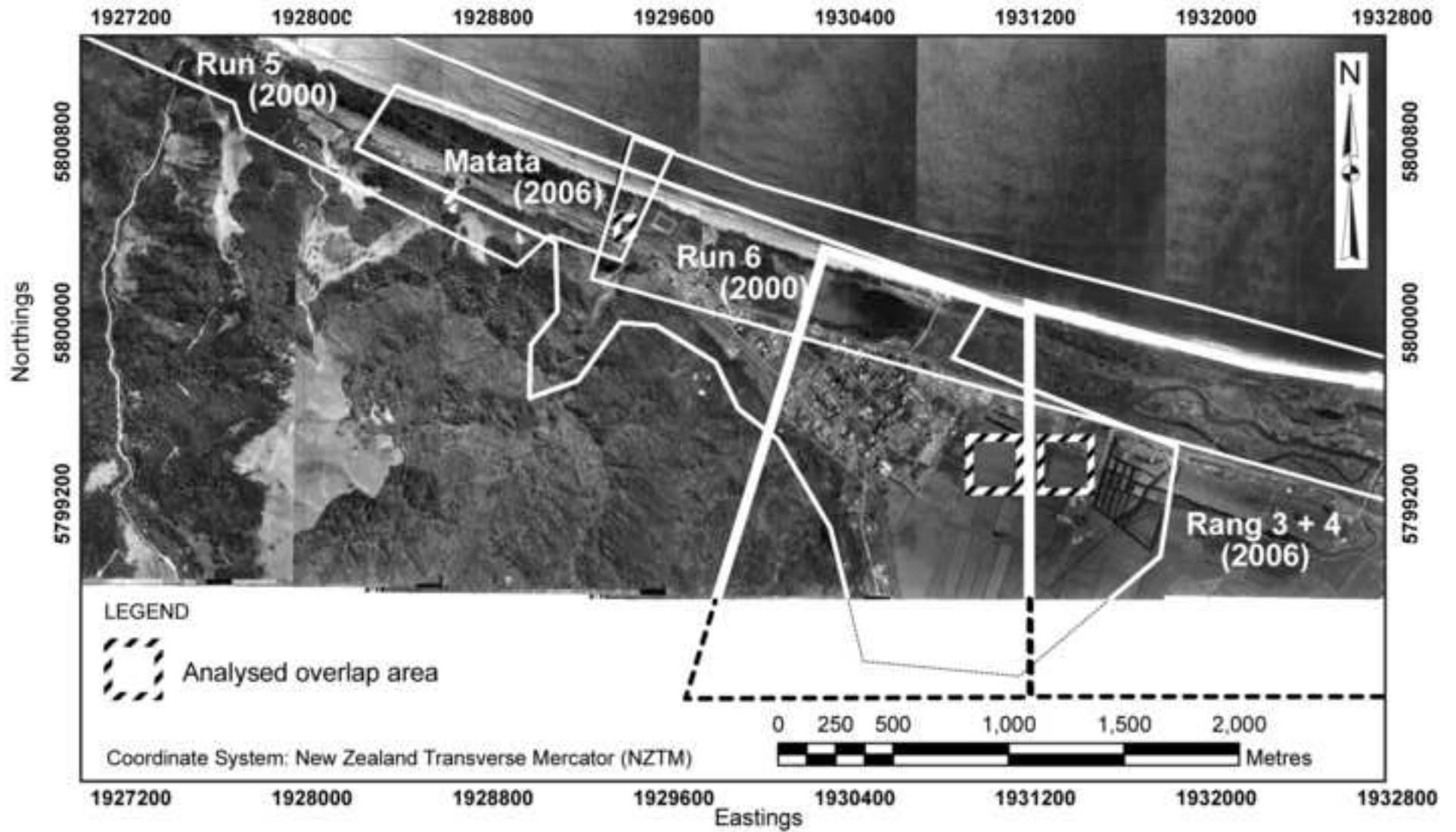
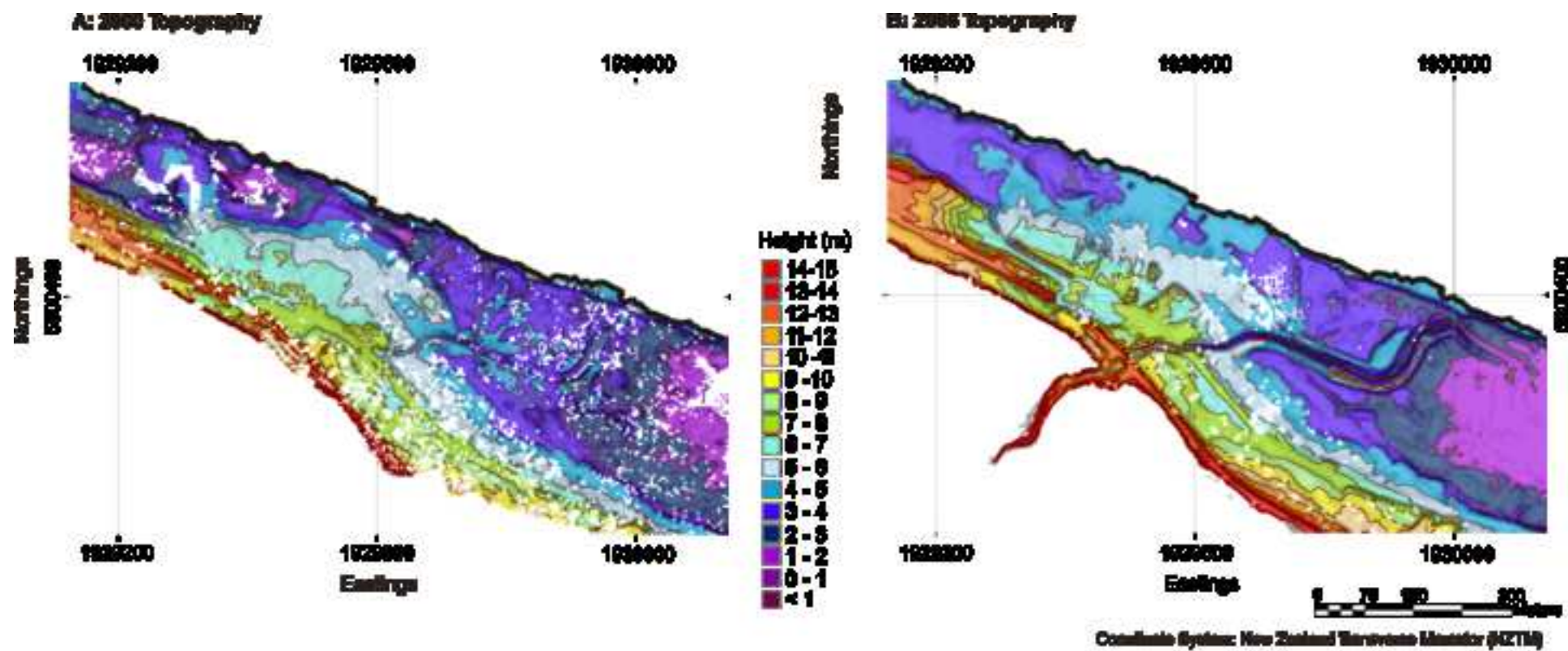


Figure8

[Click here to download high resolution image](#)



**Fig. 8. Composite figures of a selected area affected by the debris flow. A: 2008 topography
B: 2005 topography. All contours at 1 m intervals.**

Figure9

[Click here to download high resolution image](#)

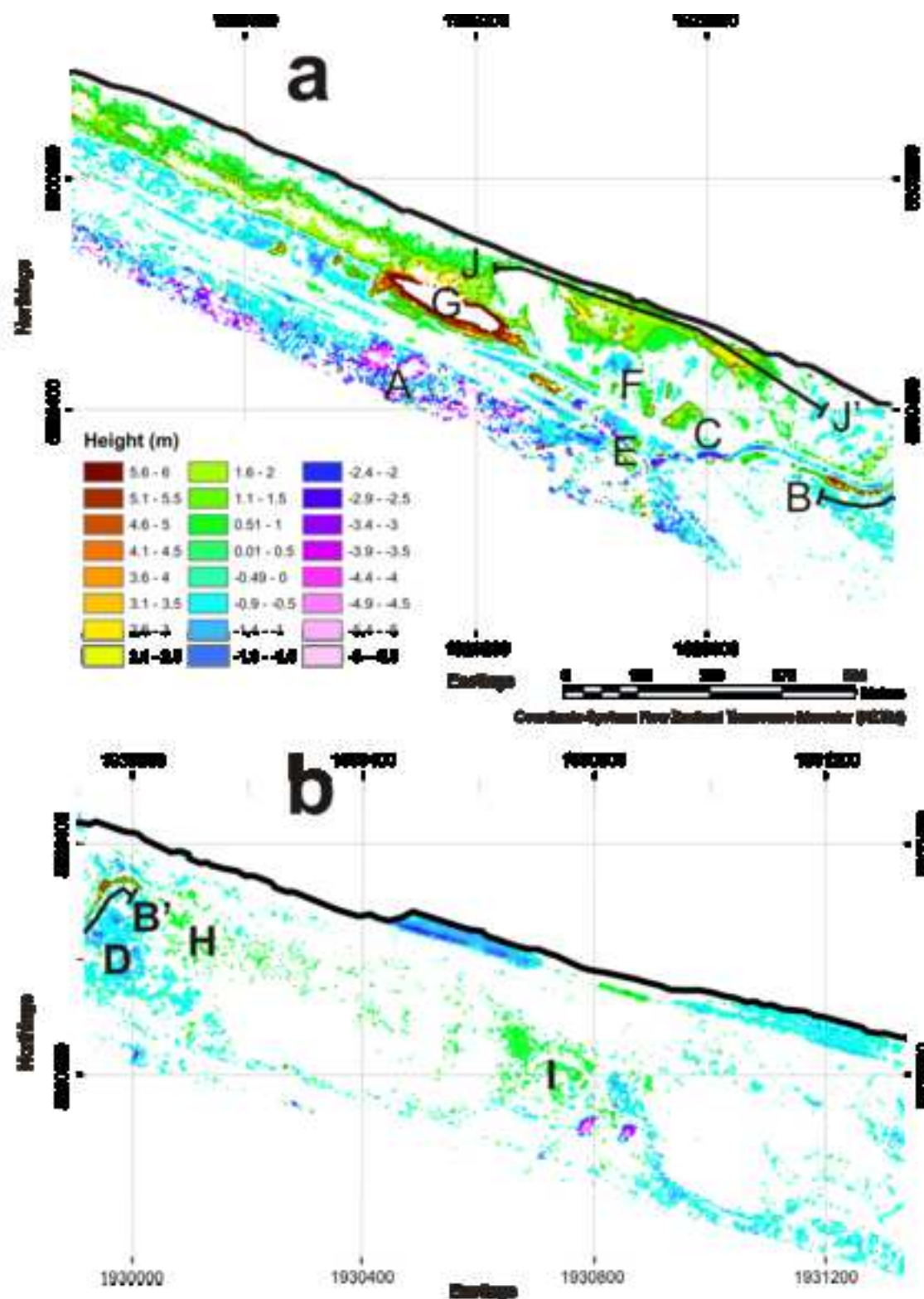


Fig. 9. Difference in vertical height between the 2000 and 2006 LIDAR data (a) for an area including the Awatururiki stream and (b) for an area to the east including Mutata lagoon (location shown in Fig. 2). Contours are at 1 m intervals. Lettered points are referred to main text. Classification of heights around the mean has resulted in high values assigned no colour, as at Point G. In this location, the maximum height is 11 m.

Figure10
[Click here to download high resolution image](#)

